International Journal of Environment and Geoinformatics (IJEGEO) is an international, multidisciplinary, peer reviewed, open access journal.

A case study on the comparison of terrestrial methods and unmanned aerial vehicle technique in landslide surveys:Sarıcaeli landslide, Çanakkale, NW Turkey

R. Cüneyt Erenoğlu and Oya Erenoğlu

RESEARCH ARTICLE

A case study on the comparison of terrestrial methods and unmanned aerial vehicle technique in landslide surveys:Sarıcaeli landslide, Çanakkale, NW Turkey

R. Cüneyt Erenoğlu[1,*] and Oya Erenoğlu[2]

[1] Çanakkale Onsekiz Mart University, Faculty of Engineering, Department of Geomatics Engineering, Çanakkale, TR

[2] Çanakkale Onsekiz Mart University, Faculty of Education, Department of Turkish and Social Sciences Education, Çanakkale, Turkey

*Corresponding author

Tel   :+ 90 286 218 0018 # 2206
E-mail   : *ceren@comu.edu.tr*

Abstract

Landslides are natural disasters with some effects in the natural environment of the Earth. A landslide has a structure that changes the natural topography boundaries by releasing the forest cover and vegetation. Heavy precipitation and seismic activities, as well as the mass movement that can be caused by landslides, trigger the possible tendency to move the soil. The formation of the current Digital Elevation model (DEM) of the area subject to landslides is important in terms of determining the direction, character and effects of the landslide. With the help of aerial photographs obtained by Unmanned Aerial Vehicle (UAV), the production of high resolution and accurate DEMs is becoming increasingly widespread. In this study, production and analysis of DEMs obtained from different dated flight data and reflecting the topography of an active landslide area were performed. Finally, it was compared with RTK-GNSS measurement results in landslide areas. According to the results obtained in the study, the production of DEM based on UAV provides higher accuracy at centimeter level. In addition, the method used is more efficient, faster and lower cost than other terrestrial techniques.

Keywords: Landslide, UAV, digital elevation model, 3D modeling, GPS-GNSS

Introduction

Natural disasters such as earthquakes, landslides, hurricanes and heavy rains affect the whole world negatively. (Sidle and Ochiai 2013). To investigate the loss of life and property caused by landslides, gradient scales and types that occur after landslides are discussed extensively. After a landslide on the earth, surface, underground and surface biomass can be changed almost completely. Landslides occurring in different locations, sizes and types have various effects on topographic structure as well as animal and plant diversity. (Garwood et al. 1979, Kaya et al., 2008; Restrepo et al. 2009; Kaya & Gazioğlu, 2015).

It is very important to determine the effects of landslides on urban areas, especially in urban areas. Geodetic, geophysical and geological methods are used to monitor and model these effects of landslides. For example, Some of the geodetic methods developed for this purpose are terrestrial surveys, GPS/GNSS technique, close range and aerial photogrammetry, satellite images and so on. On the other hand, Unmanned Aerial Vehicles (UAV) technology has been widely used because of its rapid, efficient and economical results for various applications thanks to the fact that it can be used as a pilotless carrier (Gazioğlu et al., 2017). The objective of this study is to generate the Digital Elevation Model (DEM) using UAV to assess the influence of the landslides. For

this purpose, the Sarıcaeli landslide was selected as study area. It is a deep seated rotational landslide, and consists of some transition zones. The production of the current DEM is vital for estimating the influence of the landslide. In addition, the changes of the amount of sliding mass depending on the point density and mass flow directions were studied using the DEM from the obtained data at different flight dates. The accuracy assessment for the orthophoto from UAV imagery and finally a comparison with the results from other surveys, i.e. RTK/GNSS and tape measurement is performed. To achieve the following tasks, this study was to design and develop a UAV system: (a) Design and implement a UAV system for real-time monitoring of active landslides. (b) Calibrate the sensors. (c) Connect sensors and geo-sensors such as GPS/GNSS, gyrocompass, pivoting mouth and digital camera. (d) RTK-GPS/GNSS and CORS surveys for Ground Control Points (GCPs). (e) Test and evaluate the system in a flight experiment. (f) Processing data, 3D modeling, analyzing and comparing the results for the deep seated rotational landslide.

Materials and Methods
Methodology

Photographs taken by high resolution digital cameras are widely used to create digital terrain models as well as digital and artificial objects. In the literature, there are many studies on three-dimensional terrain modeling techniques and applications. (Brown, 2003; Dequal & Lingua, 2004; Barazzetti et al., 2008; Gazioğlu et al., 2014). As is known, UAV images are used especially in the production of high resolution digital height models and city models (Greiwe et al., 2013;Gruen et al., 2013). Stereo image processing was performed for submarine ecological studies (Shortis et al., 2009). Image acquisition is a basic process for this study. A process in which information is extracted from the image sequence is the basis of image-based 3D modeling. (Avdan, et al., 2015; Erenoglu et al., 2014; Cömert et al., 2018). Although video recording is recommended as a more economical solution for a large area, photographing is always advantageous in terms of resolution (Singh et.al 2013).

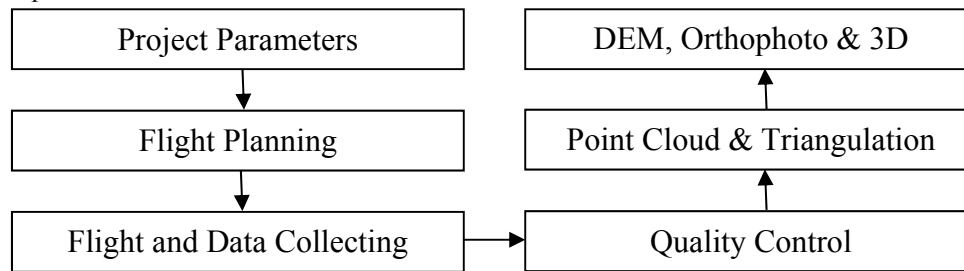| Project Parameters	DEM, Orthophoto & 3D
Flight Planning	Point Cloud & Triangulation
Flight and Data Collecting	Quality Control

Fig.1. Workflow used in this study.

Figure 1 shows the workflow used in this study. This workflow includes photogrammetric flight planning, calibration steps, and image acquisition, and quality control, data processing and model generation steps. the formation. This workflow can be easily adapted to three-dimensional modeling studies using photogrammetric data.

Unmanned Aerial Vehicle (UAV)
DJI Inspire 1 was used as carrier platform. It was preferred due to its stability during flight with reduced vibration comparing to conventional multi-copters. The default configuration nearly allowed approximately 20 minutes of the optimum flight time. The technical specifications of DJI Inspire 1 can be seen in Table 1.

Digital Camera- Systems
For optimum flight time, the DJI Inspire 1 UAV is equipped with lightweight DJI Zenmuse X3 digital camera. For all flights the camera settings were fixed to ISO 200 at F 2.8 and a focus of 20 mm. These settings enabled an average shutter speed of 1/800 s which was necessary to avoid blurred photographs. Note that a shutter is used by remote control.

Calibration Scheme

In order to calibrate DJI Zenmuse X3 digital camera, the procedure of the PhotoModeler Scanner software tool is used. for producing 3D modeling. It consists of a developed camera calibration function that defines information about the used camera that improves accuracy for the modeling studies.

It can easily calculate principal point, focal length, lens distortion and format aspect ratio of the camera. For camera calibration, we used flat sheets of target dots by taking the photos of straight, right oblique, left oblique from four different directions. The calibration process is successfully performed with a total of 20 photos. Finally, the PhotoModeler Scanner generated of a file including the calibration parameters, that are focal length, format size, principal point and radial and decentering distortion of the lens.

Table 1. The technical specifications of the DJI Inspire 1.

Weight	6.27 lbs (2845 g, including propellers and battery, without gimbal and camera)
	6.74 lbs (3060 g, including propellers, battery and Zenmuse X3)
GPS Hovering Accuracy	Vertical: ±1.64 feet (0.5 m)
	Horizontal: ±8.20 feet (2.5 m)
Max Angular Velocity	Pitch: 300°/s
	Yaw: 150°/s
Max Tilt Angle	35°
Max Ascent Speed	16.4 ft/s (5 m/s)
Max Descent Speed	13.1 ft/s (4 m/s)
Max Speed	49 mph or 79 kph (ATTI mode, no wind)
Max Takeoff Sea Level	1.55 mi (2500 m)
	2.8 mi (4500 m with specially-designed propeller)
Max Wind Speed Resistance	10 m/s
Max Flight Time	Approx. 18 min
Motor Model	DJI 3510H
Propeller Model	DJI 1345T
Indoor Hovering	Enabled by default
Operating Temperature	14° to 104° F (-10° to 40° C)
Diagonal Distance(propeller excluded)	22.8 inch (581 mm, Landing Mode)
Max Takeoff Weight	7.71 lbs(3500 g)

Study Area and Geological Features

Sarıcaeli Landslide which takes place in Sarıcaeli village of Çanakkale province is located at the coordinates of 40 ° 7 '14.48' 'K - 26 ° 26' 0.94 " D. The area is approximately 100 m above sea level. The landslide is a deep seated rotational type and is 1 km from Sarıcaeli village center and 7 km from Çanakkale city center. The width of the landslide is about 150 m and its length is about 45 m (Fig. 2). Also, Figure 3 shows the current photographs from the landslide workspace.
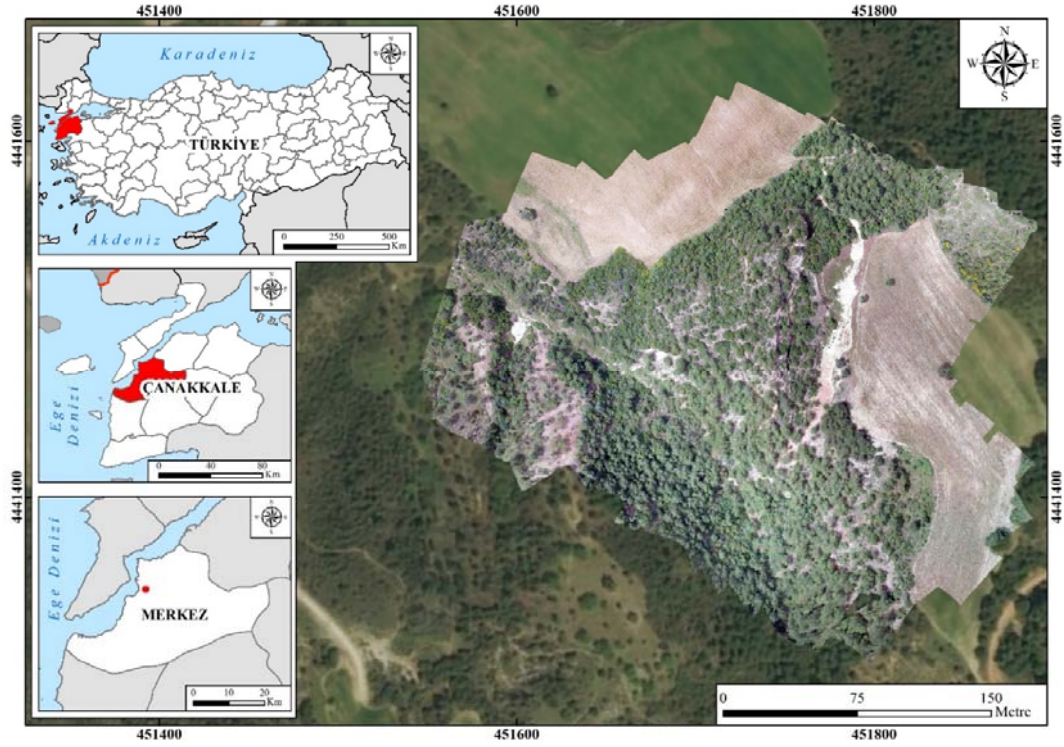
Fig. 2. Location map of the study area.

Fig. 3. Some photographs from the landslide workspace.

Volcanic and sedimentary rock assemblages constitute the geology of the study area and its surroundings (Fig. 3). Basically, Eocene-Oligocene volcanic rocks are located. These units are unconformably overlain by the sediments of the Kirazli and Camrakdere members of the Çanakkale formation. The Upper Miocene marine sediments on the both shores of the Dardanelles were first described by Şentürk and Karaköse (1987) as Çanakkale Formation. Kirazlı member of the landslide consists of small-coarse grained sandstone and pebbly conglomerate and siltstone marine units. Quartz and mica grains form the components of the sandstones. Pebbles have well developed planar parallel layers. All these sediments are affected by storm and tidal processes as well as normal wave and current processes prevailing during the deposition and the sediments are processed depending on these processes (Ilgar et al., 2008).
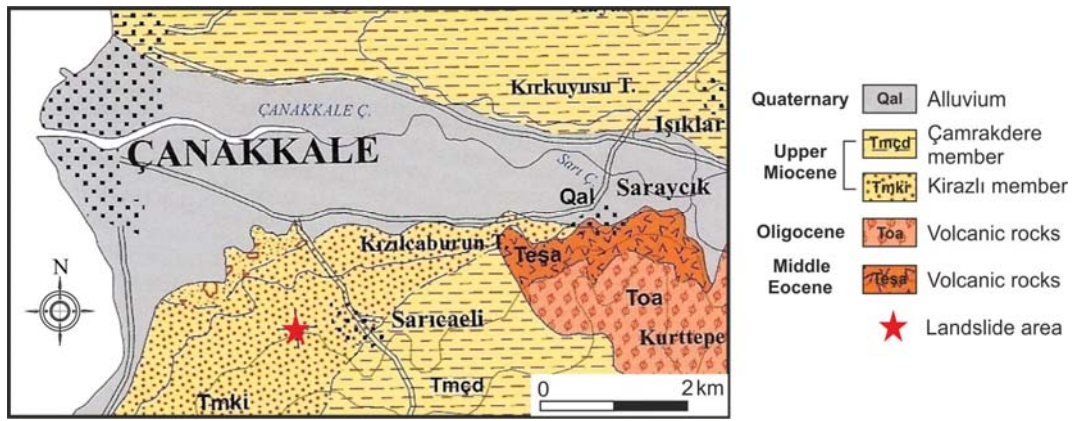
Fig. 4. The geological map of study area.

Data Acquisition / Photogrammetric Flight

DJI Inspire 1 used to fly in an autonomous mode. Before flight mission the operator needs to test all the electronic parts of UAV whether every part is working properly. For a successful flight operation, it is very critical to be aware of potential problems on UAV. It is required that the GPS onboard, rudder, elevator and main frame, digital camera, camera mount, propeller, electronic speed controller and remote controller should be checked before the flight. A suitable location is provided for launching operation after all tests have been performed. Note that the autonomous flight mission was preferred to capture images by digital camera in this study.

In this study, the operator was responsible to control UAV during launching for avoiding any damages on UAV and landing operation and to monitor flight line, data link between UAV and computer, number of satellite, real time battery status, UAV position and attitude. For flight planning step, the working area and suitable locations for starting and landing were chosen. Field studies were carried out on 30 May 2016, 6 September 2016 and 27 January 2017. All the processes described above in the data collection stage are the same for all epochs.

RTK/GNSS Surveying for Ground Control Points

For the process of geo-referencing an image to be produced, the landslide area was covered with 5 Ground Control Points (GCP) for each flight date. These points that are used to project 3D landslide model into local coordinate system were marked with plus-shaped. For this purpose, CHC geodetic GPS / GNSS receiver were used. In addition, these 5 GCPs were employed to perform accuracy assessment of UAV based 3D modeling by comparing the results from GPS/GNSS and terrestrial surveys. The RTK/GNSS surveyings were also done for collecting the landslide GCPs in order to obtain their 3D coordinates. The GCPs to be used in the image processing phase are located at the upper limit of landslides. The GCPs and their positions have been selected to be easily visible on images collected with UAV. The installed GCPs coordinates were measured in millimeter with GPS / GNSS receiver. GCPs are used in geographic referencing and datum transformations of generated SYMs and orthomosaics. GCPs coordinates were measured in the Universal Transverse Mercator 3 ° (UTM) Projection System, International Terrestrial Reference Frame 1996 (ITRF96) Datum. The slice number is 27.

Data Processing and Results

In this study, all acquired images were in good quality and they were being preceded for the processing. During the flight there was not a considerable wind, approximately 3 m/s. Note that some quality problem may be arisen due to color balancing error and blurring image during flight operation. A new flight would be planned to be performed if the quality of the images were bad. The process of 3D modelling consists of stages of interior orientation, relative orientation, aerial triangulation and bundle adjustment. Herein, three individual data were

obtained for on three different flight dates, however but only a part of the results are presented due to the lack of space.

The interior orientation was successfully defined in the camera calibration stage mentioned before the image processing. Image correlation was used as relative orientation for transferring the tie points between images. In order to align all images taken during UAV flight in the same condition, tie points were utilized. After data acquisition, the next step is image 3D data processing. In order to product 3D digital terrain model of the landslide, the UAV images were processed using PhotoModeler Scanner Software (EOS Systems). It has been well developed for all the stage of image processing such as camera calibration, triangulating image blocks using measured tie points, digitizing and texturing 3D features.

First, all photos were processed to get the image planes from UAV photos and the image frustum plane. As shown the image plane and image plane frustums, the linear path are almost parallel to each other. The camera's principal axis is the line perpendicular to the image plane that passes through the pinhole. Its intersection with the image plane is referred to as the "principal point". Image plan frustum is the region of space in the modeled world that may appear on the screen; it is the field of view of the used camera. Using the distortion functions obtained with the pre-calibration, all the photos were re-sampled. Thus, more realistic terrain view was rectified after distortion correction.

After the relative orientation process, the white point cloud and single color mesh models of the landslide were produced in the PhotoModeler Scanner software. Note that some areas in white point cloud are missing in single color mesh. The inconsistent data is automatically missed, so that the produced model can then be fitted more accurately to the input data.

Then, 3D point clouds with exact color from photos were obtained. Here, the number of point cloud significantly increased using more efficient methods of feature matching techniques. It produces more details of the landslide than the white point cloud and single color mesh. After the procedures of adjustment and projection to the UTM system using the GCPs, a surface was generated based on the 3D points after edition and noise filtering by the software. Sparse point cloud and dense point cloud can be seen in Fig. 5 respectively. Univariate statistics of the point cloud were studied in order to find out the statistical properties of the obtained data. Each coordinate component was taken as a separate data point. The autocorrelation procedure of the PhotoModeler Scanner provided a well distributed data due to normal distributed point positions of data cloud. DEM was produced using the procedure of regular grid since the triangle surface points have some irregular concentrations (Fig. 6). Note that the new surface was interpolated for all points in each 0.10 m by the radial basis function (Webster and Oliver, 1990).
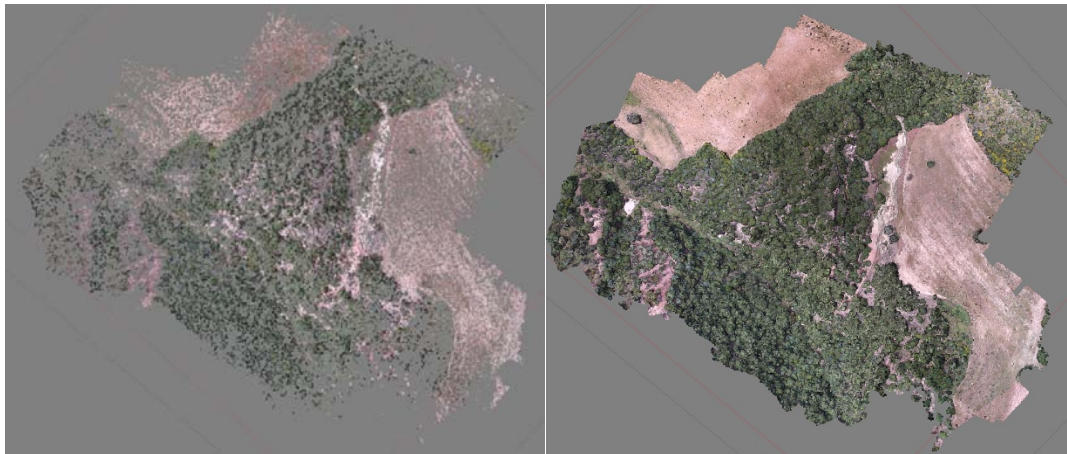

Fig. 5. Sparse point cloud and dense point cloud.

330

The obtained models were presented only for the flight at 50 m height due to the lack of space. In addition, the similar workflow is applied to the data for the other flight heights, i.e. 80 m and 30 m. Different spatial resolutions were obtained at different flight heights as accuracy criteria about the level of detail of the orthophotos generated in this study. Note that the results of the geometric accuracy assessment based on the locations of the ground control points surveyed in the field work. The Root Mean Squared Errors (RMSE) and standard deviations are 0.27 ± 0.13 for 80 m, 0.22 ± 0.11 for 50 m and 0.18 ± 0.12 for 30 m in centimeter level. As a result, the lower flight height provided higher accurate orthophoto product using a low cost UAV and camera system. Three individual DEMs were generated for three different flight dates. The final analysis of this study involves volume determination of landslide and soil loss. In general, the soil loss in the landslide area can be calculated by subtracting DEMs obtained from the data at different dates. Surface volume tools are available in ArcGIS 9.3 for calculating surface volume automatically. In order to make calculated by subtracting the three different surface volumes for the main scarp of the Sarıcaeli Landslide (Fig. 6). The results from ArcGIS 9.3 showed that the sum of soil loss of the Sarıcaeli Landslide is 6.45 m³ and the area of landslide is 1.3841 m² in the area between the 1st and 2nd surveying epochs. Fig 7 shows the visualization of differences in DEM between the 1st and 2nd surveying epochs, and between the 2nd and 3rd surveying epochs, respectively. it is clear that there is an increasing amount of soil mass change from the first epoch to the third epoch.
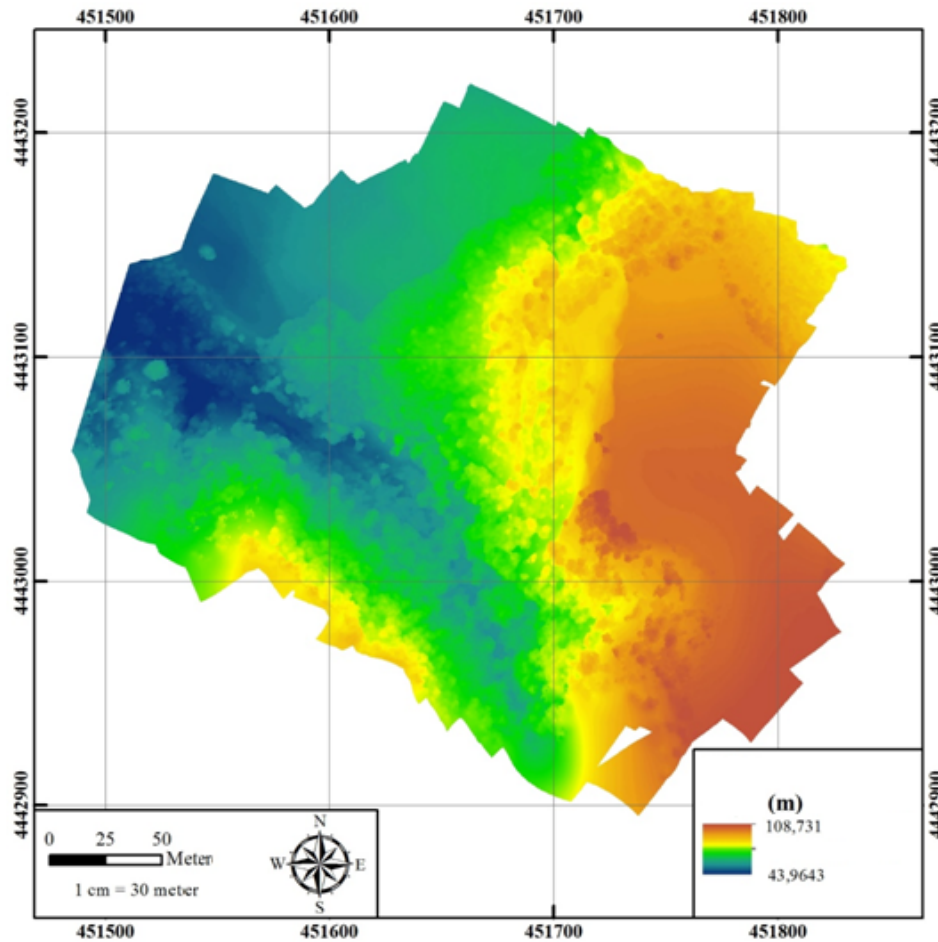

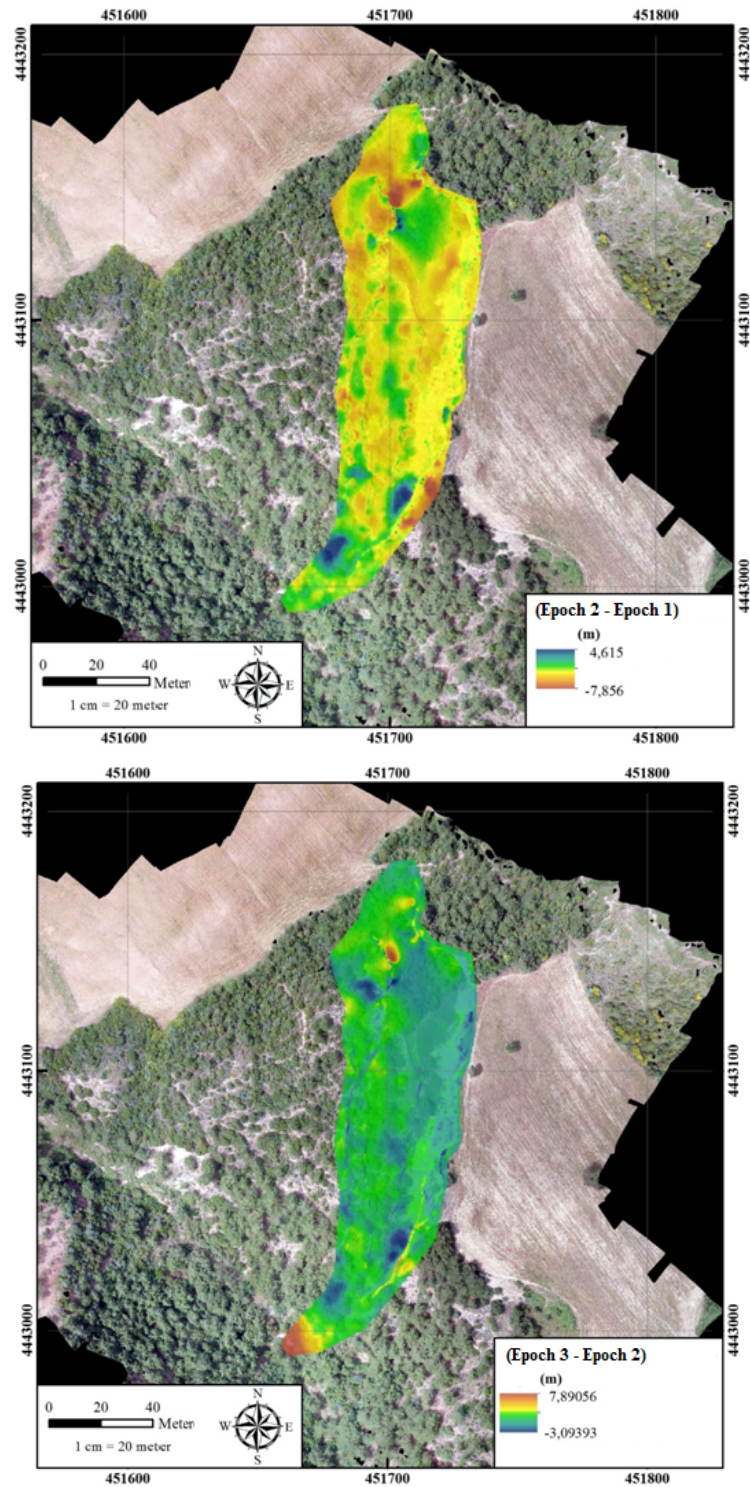Fig. 6. Digital elevation model for May 30, 2016.

Figure 7. Flow direction of soil loss in the Sarıcaeli Landslide between the 1st and 2nd surveying epochs (at left side) and between the 2nd and 3rd surveying epochs (at right side).

Discussion

The accuracy and quality assessment are performed for UAV -based products by comparing control measurements made with RTK/GNSS measurements. The orthomosaic was realized using the texture of the 3D landslide model (Fig. 8).

Figure 8. Orthomosaic model for May 30, 2016.

Table 2. The surveyed errors between UAV-product and RTK/GNSS for the GCPs.

GCP number	XY error (m)	Z error (m)
1	0.019	0.41
2	0.035	0.65
3	0.025	0.36
4	0.019	0.45
5	0.028	0.39

For this purpose, the planar and vertical comparisons are performed by control surveys of ground control points that are clearly identifiable on orthophotos. The statistics of these differences are used to evaluate the accuracy of UAV-based products. The 3D coordinates of each of the 5 GCPs were computed from UAV-based orthophoto and compared with the coordinates surveyed with RTK/GNSS. The UAV-model coordinates were derived from the producing geo-referenced orthophoto. The difference between UAV-orthophoto coordinates and RTK/GNSS coordinates of the 5 GCPs is shown in Table 2.

5 GCPs were established and surveyed by UAV- technology and also RTK/GNSS to determine the accuracy assessment. Table 5 shows the coordinates of these GCPs obtained by these methods. Then, the Root Mean Squares (RMS) were computed for X, Y, Z coordinates, respectively, by:

$$RMS_X = \sqrt{\frac{1}{n}\sum_{i=1}^{n}(X_{ORTHO_i} - X_{RTK_i})^2} \qquad \text{Eq.1}$$

$$RMS_Y = \sqrt{\frac{1}{n}\sum_{i=1}^{n}(Y_{ORTHO_i} - Y_{RTK_i})^2} \qquad \text{Eq.2}$$

$$RMS_Z = \sqrt{\frac{1}{n}\sum_{i=1}^{n}(Z_{ORTHO_i} - Z_{RTK_i})^2} \qquad \text{Eq.3}$$

The RMS values are obtained as 11.5 mm, 13.5 mm and 18.5 mm for X, Y and Z coordinates, respectively. It is clear that the coordinates obtained from UAV- orthophoto and RTK/GNSS are highly consistent in centimeter level with each other.

Finally, it is aimed to use a local measurement technique which does not take into account the systematic errors that may arise from GPS / GNSS technique. For this purpose, the distance between ground control points is taken from the produced UAV model. These distances were also measured with a steel measuring tape and the numerical values obtained with both techniques were compared with each other. The

lengths of distances obtained by both approaches can be seen at Table 3.

When the results obtained are examined, it is clear that the UAV model product and the distances obtained by the ground direction are almost close to each other. They are different from each other at most centimeters, up to 3 cm. As a result, it is clear that the UAV-assisted model products obtained from an active landslide zone close to the residential areas have sufficient accuracy when compared to the GPS/GNSS and other terrestrial methods used for point position accuracy. Therefore, the use of UAV-based techniques to model active landslides is important in terms of accuracy, efficiency and economy.

Conclusions

This study has been carried out to show that mobile platform using UAV could provide the similar result of DTM and ortho-products by comparing the ones from GPS/GNSS and terrestrial technique. The obtained results have been analyzed using root mean square error (RMSE). With the help of technology and workflow used in this study, UAV can solve many problems for various applications especially for small areas. The UAV platform used offers fast solutions for projects with limited budgets without compromising accuracy. In addition, this technology can be adopted in photogrammetric surveys that are based on modeling and monitoring based on updating information in a short time. On the other hand, this study also proves that it can be applied for low-cost landslide mapping and after-landslide event to determine area and volume loss. The outputs produced from this technology can be used by any institution or ministry concerned with environmental studies to monitor all kinds of natural disasters. For future studies, this research will be used with fixed-wing UAV, different evaluation strategies and software.

Table 3. These distances from UAV-product and a steel measuring tape.

Distance	UAV-model Measurement (m)	Steel Type Measurement (m)	Difference (m)
GCP$_1$-GCP$_2$	2.94	2.95	0.01
GCP$_1$-GCP$_3$	13.36	13.34	0.02
GCP$_1$-GCP$_4$	7.14	7.16	0.02
GCP$_1$-GCP$_5$	16.23	16.25	0.02
GCP$_2$-GCP$_3$	6.91	6.91	0.00
GCP$_2$-GCP$_4$	8.58	8.58	0.00
GCP$_2$-GCP$_5$	12.54	12.56	0.02
GCP$_3$-GCP$_4$	15.93	15.92	0.01
GCP$_3$-GCP$_5$	14.40	14.42	0.02
GCP$_4$-GCP$_5$	5.71	5.71	0.00

References

Avdan, U., Görüm, T., Cömert, R.& Nefeslioğlu, H. (2015). Sensitivity analyses for the DTMs derived from Unmanned Aerial Vehicle (UAV) in gully erosion mapping: Nallihan badland area (Ankara, Turkey), *2015 EGU General Assembly Conference*

Barazzetti, L., Brovelli, M. & Scaioni, M. (2008). Generation of true-orthophotos with LiDAR dense digital surface models, The Photogrammetric *Journal of Finland* 21(1): 26-34.

Brown, J. (2003). Aspects on true-orthophoto production. *In Proceedings of the Phot. Week'03.Wichmann,* Stuttgart, Germany 2003: 205-214.

Cömert, R., Avdan, U. & Görüm, T. (2018). Rapid Mapping Of Forested Landslide From Ultra-High Resolution Unmanned Aerial Vehicle Data, *The International Archives of the Photogrammetry, Remote Sensing and Spatial Information Sciences, Volume XLII-3/W4, GeoInformation For Disaster Management (Gi4DM),* 171-176.

Dequal, S., Lingua, A., 2004: True orthophoto of the whole town of Turin, International Archives of Photogrammetry, *Remote Sensing and Spatial Information Sciences* 34(5/C15): 263-268.

Erenoglu R. C., Akcay O. & Erenoglu O. (2015). Estimating of landslide by repeated GPS/GNSS measurements in the Ambaroba Region, Canakkale, NW Turkey. *In Proceedings of the International Symposium on Modern Technologies, Education and Professional Practice in Geodesy and Related Fields,* Sofia, Bulgaria 2015.

Erenoglu, R. C., Akcay, O., Erenoglu, O., Uluocak, E. S. & Karaca, Z. (2014). UAV based monitoring of Adatepe Landslide, Canakkale, NW Turkey. *In Proceedings of the FIG Congress 2014, Engaging the Challenges, Enhancing the Relevance,* Kuala Lumpur, Malaysia 2014.

Ilgar, A., Sezen Demirci, E., Duru, M., Pehlivan, Ş., Dönmez, M. & Akçay, A. E. (2008). 1/100000 ölçekli Türkiye Jeoloji Haritaları, Çanakkale H15 ve H16 Paftaları. *MTA, No:100*

Garwood, N. C. et al., 1979: Earthquake-caused landslides: a major disturbance in tropical forests, *Science* 205: 997–999.

Gazioğlu, C., Alpar, B., Yücel, ZY., Müftüoğlu, AE., Güneysu, C., Ertek, TA, Demir, V. & Kaya, H. (2014). Morphologic Features of Kapıdağ Peninsula and its Coasts (NWTurkey) using by Remote Sensing and DTM. *International Journal of Environment and Geoinformatics (IJEGEO)*, Vol. 1(1): 48-63.

Gazioğlu, C., Varol, ÖE., Şeker, DZ. & Çağlar, N. (2017). Determination of the Environmental Impacts of Marine Accidents

Using UAV and RS Technologies, *19th MESAEP Symposium on Environmental and Health Inequity, Roma, ITALYA, 3-6 Dec 2017.*

Greiwe, A. & Gehrke, R. (2013). Foveon Chip oder Bayer Pattern - geeignete Sensoren zur Aerophotogrammetriemit AUS. *In: Photogrammetrie, Laserscanning, Optische 3D-Messtechnik -Beiträge der Oldenburger 3D-Tage 2013* (Luhmann,T., Müller, C., ed.): 334-343.

Gruen, A., Huang,X., Qin,R., Du,T.,Fang,W.,Boavida,J. & Oliveira, A. (2013). Joint processing Generating a Digital Elevation Model using Unmanned Aerial System... Seite 61 of UAV imagery and terrestrial mobile mapping system data for very high resolution city modeling, *ISPRS-International Archives of the Photogrammetry, Remote Sensing and Spatial Information Sciences* 1(2): 175 - 182.

Kaya, H., & Gazioğlu, C. (2015). Real estate development at landslides. *International Journal of Environment and Geoinformatics (IJEGEO)*, 2(1): 62–71.

Kaya, H., Yücel, Z. Y., Doğan, E. & Gazioğlu, C., (2008). İstanbul'un Marmara Denizi Kıyılarında Heyelan Risk. *Türkiye' nin Kıyı ve Deniz Alanları VII. Ulusal konferansı, Türkiye Kıyıları 07 Konferans Bildirileri Kitabı,* 986–97.

Restrepo, C. et al., 2009:Landslidingandits multi-scaleinfluences on mountainscapes, *BioScience* 59:685-698.

Shortis, M., Harvey, E. S. & Abdo, D. (2009). A review of underwaterstereo-image measurement for marine biology and ecology applications, *Oceanogr Mar Biol AnnuRev* 47: 257-292.

Sidle, R. C. & Ochiai, H. (2013). Landslides: processes, prediction, andlanduse, *Water Resources Monograph 18.* Washington, DC: American Geophysical Union.

Singh, R., Qureshi, Q., Sankar, K., Krausman, P. R. & Goyal, S. P. (2013). Use of camera traps to determine dispersal of tigers in semi-arid landscape, western India, *J Arid Environ* 98: 105-108.

Şentürk, K. & Karaköse, C. (1987). Çanakkale boğazı ve dolayının jeolojisi. *MTA Rapor no: 371* (unpublished)

Webster, R. & Oliver, M. A. (1990). *Statistical methods in soil and land resources survey,* Oxford University Press.